Colloids and Surfaces, 4 (1982) 285—303
Elsevier Scientific Publishing Company, Amsterdam — Printed in The Netherlands

SMALL ANGLE X-RAY SCATTERING FROM COAL-DERIVED LIQUIDS

BENEDICT HO* and DALE E. BRIGGS

Department of Chemical Engineering, University of Michigan, Ann Arbor, MI 48109 (U.S.A.)

(Received December 30th, 1981; accepted January 4th, 1982)

ABSTRACT

Small angle X-ray scattering measurements were used to determine the size and shape of asphaltene and preasphaltene micelles in solution. The fraction of the coal-derived liquids forming micelles in solution was as high as 49%. The fraction depends upon the concentration and molecular size of the asphaltenes and preasphaltenes, the $\pi-\pi$ and/or hydrogen bonding properties of the solvent and the agitation. Most systems studied were polydispersed with the majority of the micelles being spherical with a diameter of 22—38 Å. Micelles in the 80—100 Å range were also apparent but at 5—12% of the number of the smaller size. Variations in the scattering intensity over the scattering angles and the variations of the absolute intensity of scattered X-rays from solutions irradiated immediately after ultrasonic agitation and upon extended sitting, suggested the presence of a low level floc in most of the solutions.

INTRODUCTION

Coal-derived liquids are complex mixtures of liquid and semi-liquid constituents. They can be broadly classified as oils, resins, asphaltenes and preasphaltenes. Oils and resins are nominally soluble in pentane, asphaltenes are insoluble in pentane but soluble in benzene or toluene and preasphaltenes are insoluble in toluene but soluble in tetrahydrofuran (THF) or pyridine. The molecular weight, number of condensed aromatic rings, the number of nitrogen, oxygen and sulfur heteroatoms and the concentration of metals increases in going from the average molecule in the oil fraction to the average molecule in the preasphaltene fraction [1]. Most of the oxygen in the asphaltene and preasphaltene fractions is phenolic oxygen and most of the nitrogen is basic ring nitrogen.

The physical state of coal-derived liquids depends significantly on the relative amounts of each fraction. Anomalies are observed when coal liquefaction slurries containing high levels of asphaltenes and preasphaltenes are filtered in the 200—320°C temperature range [2]. The anomalies have been attri-

*Current address: AMOCO Production, Tulsa, Oklahoma.

0166-6622/82/0000—0000/$02.75

buted to the presence or formation of colloidal-size particles and flocs in the system.

Colloidal-size particles can form from the association of asphaltene and preasphaltene molecules through $\pi-\pi$ and hydrogen bonding. Snyder [3] showed that the free energy of adsorption, ΔG, for adsorption of aromatic amines from pentane onto water-deactivated alumina was a linear function of the number of π electrons when the amino group was in the position of minimum steric hindrance. Therefore strong attractive forces would be expected to exist between molecules in the asphaltene and preasphaltene fractions. These forces could result in intermolecular associations in the 200—320°C temperature range. Differences in molecular structure between associated molecules can produce a residual attraction for other molecules. Depending upon the magnitude of the residual attractive force, three or four polyaromatic molecules could associate into a stacked arrangement to form a nominally spherical colloidal-size particle. Pyridine and phenol can associate through $\pi-\pi$ bonding and hydrogen bonding in the orientation illustrated in Fig. 1. The association results in a residual dipole and the associated pair is not precluded from further association, although the force for association would be less. Associations as illustrated in Fig. 2 would be expected.

An attractive force to a lesser extent is the London—Van der Waals electromagnetic (cohesion) force. This force becomes more significant between particles and clusters as the attraction between atom pairs is additive. The summation leads not only to a total larger force but also to a less rapid decay with increasing distance of separation. Although London—Van der Waals forces would not be expected to cause molecular associations, they could cause associations between colloidal-size particles of the type illustrated in Fig. 2.

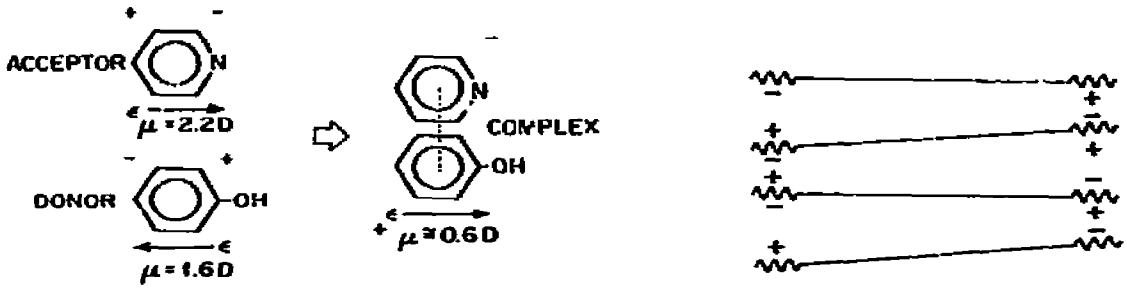

Fig. 1. Illustration of $\pi-\pi$ bonding between phenol and pyridine.

Fig. 2. Ideal stacking arrangement for aromatic sheets into a nominally spherical micelle.

In addition to possible electrostatic repulsions which result from certain orientations of molecules with respect to each other, two other repulsive forces exist in coal-derived liquids. These forces inhibit intermolecular association and promote stability to those colloidal particles that do form. Entropic repulsion (steric hindrance) is associated with long chain groups

substituted into the principal molecular structure. When molecules or particles with long chains approach, the steric hindrance greatly limits freedom of movement of the projecting chains and limits the distance of approach between molecules. Alkyl groups are common in the aromatic structure of coal-derived liquids. Solvation repulsion arises with approaching molecules, or particles "squeeze out" the solvent molecules between them. When the solvent is polar or contains a high concentration of polar compounds, coagulation of particles or association of molecules becomes less probable because more energy must be expended to "squeeze out" the solvent. Resins and low molecular asphaltenes would be expected to limit associations between asphaltenes and would promote stability of any colloidal particles that did form.

The small angle X-ray technique was selected to study the physical state of selected fractions of coal-derived liquids when dissolved or dispersed in different solvents. The technique is particularly effective for the size of the colloidal particles expected in the system studied. Unfortunately, the method has some limitations. When particles > 1000 Å exist or form in the system, Mie scattering attenuates the X-ray signal and produces a periodicity in the X-ray intensity in the small angle range of interest. Multiple scattering can cause X-ray attenuation when the concentration of scattering particles becomes large. An underestimate of the colloidal system results. Although it is possible to design and operate a small X-ray cell at elevated pressures and temperatures, it is extremely difficult. A small angle X-ray cell was constructed to examine samples at 70°F. Sample concentrations were selected to avoid or minimize multiple scattering.

SAMPLE PREPARATION

Coal-derived liquids from the vacuum bottoms produced from the liquefaction of an Illinois No. 6 coal in the H-Coal process were separated into four fractions by sequential batch solvent extractions. The extracts were separated from the residue by filtration through Whatman No. 42 (2 μm pore size) paper. Details on the extraction procedure, the method of solvent removal and the analytical methods mentioned below are given in ref. 4. Using pentane, a mixture of 75 vol.% pentane/25 vol.% toluene, toluene and THF, the vacuum bottoms were separated into pentane-soluble oils and resins, pentane-insoluble, 75 vol.% pentane/25 vol.% toluene-soluble low molecular weight asphaltenes, 75 vol.% pentane/25 vol.% toluene-insoluble, toluene-soluble high molecular weight asphaltenes, and toluene-insoluble, THF-soluble preasphaltenes. The high molecular weight asphaltenes and preasphaltenes were referred to as TS and THF material, respectively. The TS material was further fractioned by preparative gel permeation chromatography (GPC) into five fractions. The column packing was 8% divinylbenzenestyrene copolymer and THF was the eluting solvent. The first fraction eluted from the GPC column was labeled GPC-1 and the fifth fraction GPC-5.

Each sample was analyzed by microcombustion analysis to determine the weight percent carbon, hydrogen, nitrogen and sulfur. Oxygen was determined by difference. The samples were also analyzed by neutron activation analysis to determine the concentration of those metals which can be determined by intermediate irradiation times. Proton NMR was used to determine the ratio of aliphatic hydrogen to aromatic hydrogen. The results of the analyses are presented in Table 1. The TS fraction was found to contain a higher than expected level of metals. A portion of the material was dissolved in THF and filtered through Whatman No. 42 paper to produce the Tsf fraction. Molecular weights were measured with a vapor pressure osmometer using pyridine at 75°C.

The number of carbon, hydrogen, nitrogen, oxygen and sulfur atoms in the "average" molecule of each fraction was estimated using the molecular weights and elemental analyses. When these numbers are taken in conjunction with the proton NMR results, differences between the fractions become readily apparent.

Although the neutron activation analyses are not very quantitative, these and other analyzes [1] show that GPC fractionation removes a substantial amount of the metals retained in the fractions isolated by solvent extraction. Those metals retained in the GPC fractions could be in organometallic molecules, as distinct mineral particles of the same approximate size as the mole-

TABLE 1

Analysis of coal-derived materials from H-Coal vacuum still bottoms

Sample	Wt. fraction	Mol. wt.	Weight percent					Atoms in average molecule					H_{aliph}/H_{ar}
			C	H	N	O[b]	S	C	H	N	O	S	
TS[a]		699	87.40	6.30	1.17	1.96	3.17						2.7
Tsf		578	88.26	6.38	1.23	3.47	0.66	42.51	36.86	0.51	1.25	0.12	1.8
THF		888	84.09	6.11	1.74	6.98	1.08	62.23	54.26	1.10	3.87	0.30	1.4
GPC-1	0.172	663	84.29	6.95	1.36	3.44	0.96	46.57	46.08	0.64	2.67	0.20	3.6
GPC-2	0.179	588	85.36	7.08	1.29	5.45	0.82	41.83	41.63	0.54	2.00	0.15	3.1
GPC-3	0.156	401	86.41	7.52	1.17	4.18	0.72	28.88	30.16	0.34	1.05	0.09	2.8
GPC-4	0.168	260	87.87	7.59	1.10	3.11	0.33	20.94	21.71	0.22	0.56	0.03	2.5
GPC-5	0.325	222	86.35	7.90	0.71	4.91	0.13	15.97	17.54	0.11	0.68	0.01	2.9
ΣGPC	1.000	402											

Metals contents from neutron activation analysis—ppm by wt.[c]

	Al	Ca	Cl	Mg	Mn	Na	Ti	V
TS	19314.9	5307.0	821.5	2103.8	103.2	1479.9	1258.3	99.4
GPC-1	57.1	< 78.2	168.3	<189.2	26.8	75.0	250.5	2.2
GPC-2	23.8	< 75.7	153.1	<164.9	17.3	40.7	130.1	1.2
GPC-3	< 10.3	< 83.9	119.6	<178.7	5.4	39.4	< 62.4	0.3
GPC-4	< 12.2	<258.6	156.9	<187.7	< 1.5	< 26.3	< 76.7	0.3
GPC-5	< 10.3	< 76.3	188.0	<143.0	< 1.0	< 14.3	< 46.7	<0.2

[a] 21.4 wt.% of the TS Sample was a reddish-gray residue and C,H,N and S were adjusted for residue.
[b] Determined by difference.
[c] Values shown as "less than" are the upper limits of determination with other elements present.

cules in the GPC fractions eluted or colloidal-size mineral particles which are associated with polyaromatic molecules in the GPC fractions. The reduction is least for manganese and titanium. It is common to see titanium retained in the asphaltene and preasphaltene fractions.

X-RAY METHODS

Equipment

The apparatus consisted of an X-ray tube and generator, a gonimeter, a sample cell and a detector. The X-ray tube was a Philips copper target micro-focus tube (No. 34048) with a beryllium-mica window having a line focus of 0.1 X 10 mm. A 0.06 mm thick nickel filter was used as a K_β filter. The generator was operated at 40 KV and 25 mA. It had a current stability of ± 0.05%.

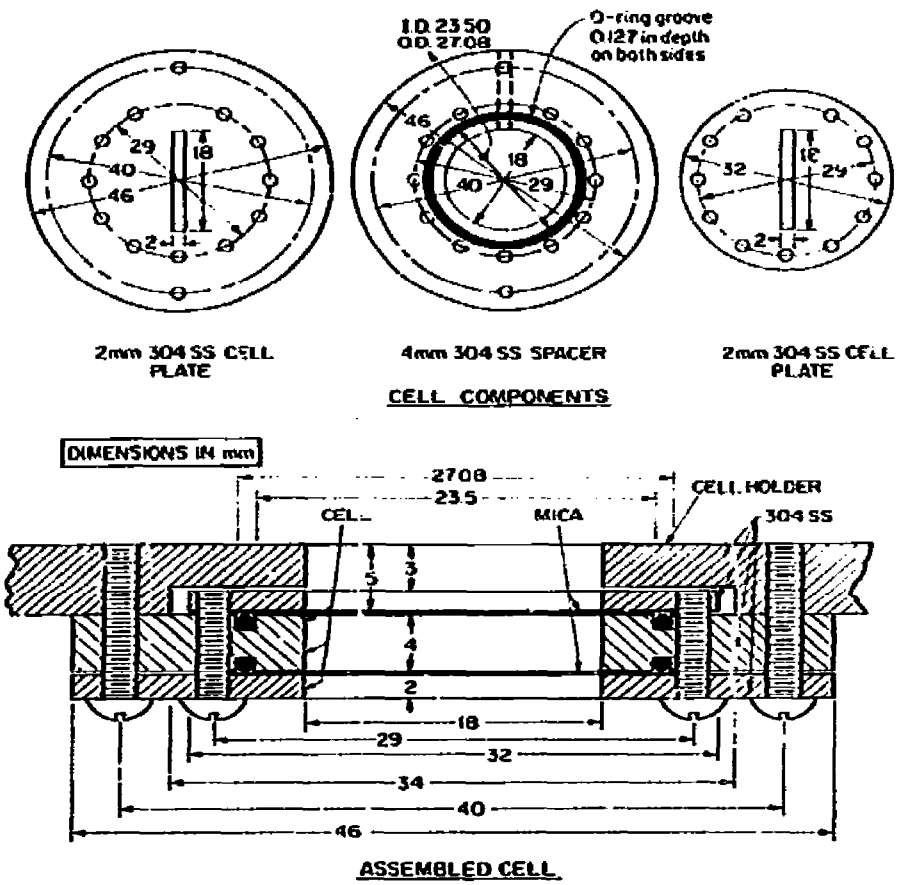

Fig. 3. Component parts and cross-section of small angle X-ray scattering cell.

The goniometer was an automated Rigaku-Denki low angle unit with five slit collimators. The step-scanning controller moved the counter bench in specified two theta scattering angle steps up to a maximum diffracted beam of 10°. Stepping in both + and − directions was possible.

A schematic drawing of the sample cell is presented in Fig. 3. The cell was constructed of type 304 stainless steel. Two Viton-A O-rings were placed on both sides of the 4-mm thick center spacer. The O-rings were seated on the two 0.06-mm thick mica windows forming an approximately 1.0 ml cavity. The cavity was filled with a hypodermic syringe through one of two small holes at the top of the center spacer.

Two detector systems were used in the study. Most of the data were taken on a system consisting of a Hewlett Packard Model 5580 A NIM power supply, Model 5554 A preamplifier, Model 5582 A linear amplifier, Model 5583 A single channel analyzer and a Model 5590 A scaler-timer. A Harshaw N-780 log/linear ratemeter and a Harrison 6110 A D.C. power supply were also a part of the system. The X-ray beam at the cell was 0.1 × 10 mm. The time to obtain 5000 counts at each step increment was automatically recorded. Counting was initiated at 0.1° and run to 2° in 0.05° intervals.

The second detector used was a Tennelec Model PSD-110 linear position sensitive gas flow proportional counter. A mixture of 10% methane in argon was supplied to the detector via a Tennelec GR-1000 gas regulator. The X-ray beam at the cell was 0.1 × 6.35 mm. The system was run for 1 h and the counts at each position accumulated in the 40-channel memory.

Corrections

The measured intensity of the scattered X-rays were corrected for background intensity. This included a correction for scatter from the X-ray collimation slits, from air in the region of the sample which was not evacuated, from the mica windows in the sample holder and from the solvent or mixtures of solvents. The method of Hendricks and Schmidt [5, 6] was used to estimate the collimation correction. Background data were obtained with the empty sample cell in place and with solvent or solvents in the cell to provide data for the other corrections.

Methods of data analysis

After the collimation and the background corrections are made to the measured intensity, the corrected X-ray intensity, $I(S)$, at the radial coordinate position, $S = 2 \sin \theta / \lambda$ is obtained. $I(S)$ represents the intensity attributed to the asphaltenes and preasphaltenes in the sample. The scattering angle is 2θ and the X-ray wavelength is $\lambda = 1.54$ Å. The data were analyzed for size distribution, volume fraction of the asphaltenes and preasphaltenes which were scattering and molecular weight of the scattering units.

Particle size for a monodisperse system

At scattering angles less than 3°, the Guinier [7] approximation for the intensity of the scattered X-ray is given by

$$I(S) = N(\Delta\rho_0)^2 V^2 \exp[-(4/3)\pi^2 R^2 S^2) \quad (1)$$

where N is the number of scatterers, $(\Delta\rho_0)^2$ is the electron density difference between the scatterers and the surroundings and V is the volume of the scatterer, R is the average radius of gyration of the particle. R is defined as the root mean square of the distances of atoms from the center of gravity of the particle, each distance being modified by a coefficient equal to the atomic number of the atom. By plotting ln $I(S)$ versus S^2 the Guinier [7] scattering plot is obtained. If the data can be correlated well with a straight line, then the system is a monodisperse system and the radius of gyration of the particle can be obtained from the Guinier scattering plot. If the particle is assumed to be spherical the diameter of the particle, d, can be estimated according to Beeman [8] from

$$d = 2\sqrt{(5/3)R^2} \quad (2)$$

Particle size distribution for a polydisperse system

If the Guinier scattering plot is curved, the system is a polydisperse system. The intensity of X-rays scattered from a polydisperse system is the sum of the intensities of scattered X-rays for the different groups of particles. The intensity of scattered radiation [7, 9] as a function of S is given by:

$$I(S) = B \int_0^{\bar{R}} W(R)R^3 \exp[-(4/3)\pi^2 R^2 S^2]dR \quad (3)$$

where B is a proportionality constant and $W(R)$ is the weight fraction of the radius of gyration R. To determine the size distribution from observed intensity data the integral must be inverted. Similarly, the total intensity of the X-rays scattered by an isotropic system of particles of the same shape but different characteristic dimension, d, is a function of the radial coordinate in reciprocal space, S. When multiple scattering can be neglected, the relationship between the total intensity and S can be expressed as an integral over the particle size range in which the distribution function, $D(d)$, is multiplied by a common single-particle scattering function of $S(d)$ which can be calculated for the assumed particle shape. The particle size estimate results from a trial-and-error procedure with adjustments made to the size distribution until the sum of the squared deviations is minimized. Vonk [10] developed the procedure and prepared a computer program to do the calculations. Vonk made the program available for this research.

An example of the corrected observed intensity of scattered X-rays from a polydisperse system is illustrated in Fig. 4. The scatter in the data as $S^2 > 1 \times 10^{-4}$ Å^{-2} is attributable to Mie scattering. The particle-size distribution for the system was obtained from the Vonk program and is presented in Fig. 5. The number distribution data are normalized to 1.0 for the size

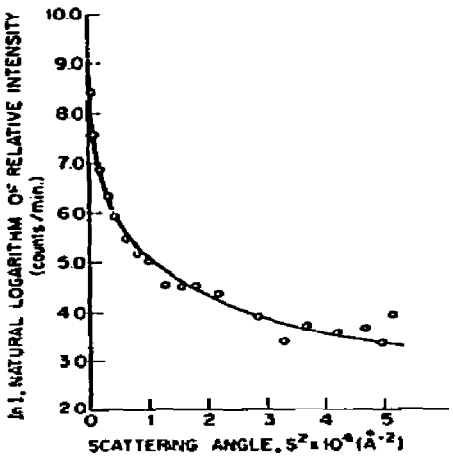

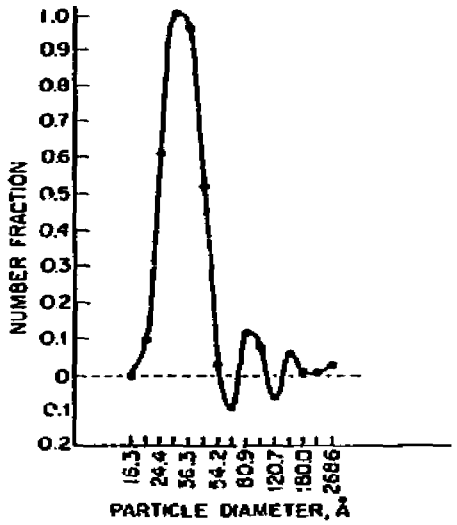

Fig. 4. Scattering intensity of toluene-soluble, 75% pentane/25% toluene-insoluble asphaltenes in mixture of 90 wt.% tetralin, 2.5 wt.% *m*-cresol and 7.5 wt.% γ-picoline at a concentration of 4 wt.% at 70°F.

Fig. 5. Particle size distribution plot of a 100% toluene-soluble, 75 vol.% pentane/25 vol.% toluene-insoluble asphaltenes at a concentration of 10 wt.% in a mixture of 90 wt.% tetralin, 2.5 wt.% *m*-cresol and 7.5 wt.% γ-picoline at 70°F.

most frequent in the system. The particles were best approximated as spheres as were all the small angle scattered X-ray data in this study. The correlation coefficient ranged from 0.8 to 0.9. The negative numbers in Fig. 5 are artifacts of the Vonk program and result in part from the Mie scattering by large particles or a floc produced by aggregation of smaller particles. This can also be attributed to the fact that the particles are not absolutely spherical.

Volume fraction of the sample scattering

The volume fraction of a sample scattering X-rays, $\Delta V/V$, was estimated from the total integrated corrected intensity in relation to the primary beam intensity, I_0, per volume irradiated using the method of Kratky [11]. The ratio of $I(S)$ to I_0 is defined as $I^i(S)$ and

$$Q_0 = \int_0^\infty S^2 I^i(S) dS = \frac{(\Delta\rho_0)^2}{4} \frac{\Delta V}{V} \qquad (4)$$

The evaluation of Q_0 was carried out by the numerical integration of the function. $\Delta\rho_0$ is the excess electron density difference between the sample that is scattering and the solvent. The electron density of the coal-derived materials was taken as 0.5 electrons per Å^3. The electron density for amorphous carbon is from 0.5 to 0.6 electrons per Å^3. The absolute intensity was measured by using a calibration sample (Lupolen No. 16/12) provided by Kratky [12].

Molecular weights

The molecular weights of the samples forming nominally monodisperse systems were estimated from the absolute intensity and the relative intensity at zero angle for each sample by the method of Kratky [12].

RESULTS

Several of the small angle X-ray measurements of Ho [4] are presented. The data were selected to give some perspective on the differences between various coal-derived liquid fractions in solution and the effect of the solvent and concentration of the fraction in a solvent on the nature of the fraction in solution.

Model compound studies were effected by Ho [4] with *o*-phenylphenol (MW = 170) and quinoline (MW = 129) to estimate the lower limit of significant small angle scatter by molecules that associate. When equal molar ratios of *o*-phenylphenol and quinoline were dissolved in tetralin, carbon tetrachloride and heptane to give concentrations from 1 to 5 wt.%, no appreciable excess intensity values could be obtained between the *o*-phenylphenol and quinoline in the solvents and the solvents. This suggests that the lower molecular weight limit for significant scatter is at least 300.

Coal-derived liquid fractions in pyridine

Small angle X-ray scattering data for the high molecular weight aspahltene (TS) and preasphaltene (THF) fractions in pyridine at a concentration of 10 wt.% are presented in Fig. 6. Both fractions result in polydispersed systems. As expected, more scatter results from the THF fraction. The high intensity from the TS fraction at the smallest angle indicates the presence of more large particles in the TS fraction than in the THF fraction. This is not surprising as the analysis of the TS fraction indicated the presence of mineral matter. The intensity from the TS filtered material, the Tsf fraction, and a filtered Tsf fraction were considerably less but still indicated the presence of polydispersed systems.

The four sets of data in Fig. 6 were analyzed using the Vonk computer program and the particle size distribution data are given in Table 2. The fraction of the irradiated volume scattering X-rays was computed from the integrated intensity and the fraction of the coal-derived material scattering X-ray was computed on the assumption that only associated coal-derived molecules are scattering X-rays. Statistically, the particles are best described as spherical particles. In each sample, three distinct peaks occured in the particle size distribution. The most prominent particle size was the smallest, the particle diameter being approximately 33 Å. The second peak occurred at approximately 89 Å with the number of particles being roughly 10% of the smaller size. The size of the largest particles ranged from 147 to 220 Å in the four fractions. Consistent with the shapes of the relative intensity

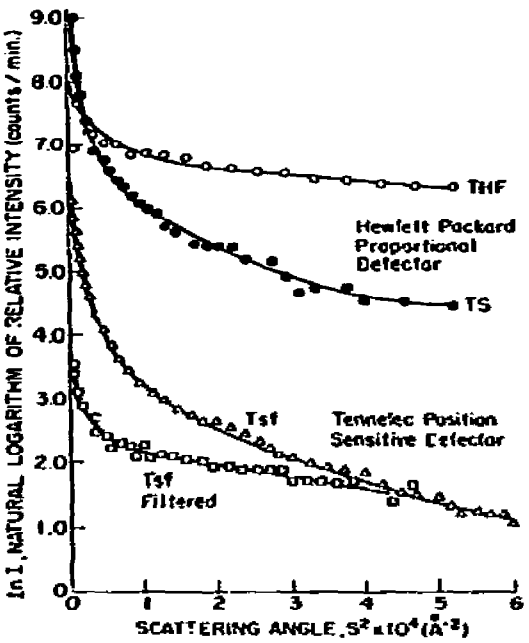

Fig. 6. Coal-derived liquid fractions at a concentration of 10 wt.% in pyridine at 70°F.

TABLE 2

Small angle X-ray scattering results for coal-derived liquid fractions in pyridine at a concentration of 10 wt.% at 70°F

Sample	THF	TS	Tsf	Tsf–f
Size 1 particle diam. Å	32.6	29.8	32.9	36.3
No. particles size 1/No. size 1	1.0	1.0	1.0	1.0
Size 2 particle diam. –Å	89.4	80.9	89.4	98.8
No. particles size 2/No. size 1	0.110	0.130	0.186	0.098
Size 3 particle diam. –Å	153.4	219.9	162.9	147.4
No particles size 3/No. size 1	0.01	0.050	0.060	0.014
Integrated intensity, $Q_e \cdot 10^5$	24.5	12.8	3.9	3.43
Vol. fraction scattering, $(\Delta V/V) \cdot 10^2$	3.895	2.200	0.0988	0.0869
Fraction of coal-derived material scattering X-ray based on 8 vol.% in pyridine	0.487	0.275	0.012	0.011

curves, relatively more large particles were present in the TS and Tsf samples.

Based on the coal-derived material occupying 8% of irradiated volume, 49Å of the preasphaltene material was present as associated molecules. As expected, the fraction in the associated state drops off to 28% for the TS fraction and to 1% when the TS fraction is filtered once or twice.

GPC-fractionated asphaltenes in pyridine and in a mixture

The TS fraction was fractionated by GPC to give five fractions with a more narrow range of molecular sizes than the TS fraction. Scattering data for the five fractions in pyridine and in a mixture of solvents at a concentration of 10 wt.% are presented in Figs. 7 and 8. The analysis of the scattering data is given in Table 3.

When dispersed in pyridine, the five fractions formed monodispersed systems. Using Guinier's approximation the size of the scattering particles was estimated to be about 22 Å in the solutions containing the GPC-4 and GPC-5 fractions and 38 Å in the solution containing GPC-1. As GPC-1 contains an aliphatic to aromatic hydrogen ratio of 3.6, the presence of alkyl side chains and the larger molecular weight would attribute to the large particle size in that fraction. The variation in the fraction of the GPC sample scattering is roughly the same as it is in Table 2 for the coal-derived liquid fractions. GPC-1 is similar to preasphaltenes and GPC-5 is similar to the Tsf asphaltenes. The weight average molecular weights were estimated from the relative intensity at zero angle. If the molecular weights determined by vapor pressure osmometry are taken as the molecular weights of the unassociated

TABLE 3

Small angle X-ray scattering results for GPC fractioned coal-derived asphaltenes in pyridine and in a mixture of solvents at a concentration of 10 wt.% at 70°F

	GPC-1	GPC-2	GPC-3	GPC-4	GPC-5
Sample in pyridine					
Radius of gyration –Å	14.8	12.9	10.7	8.3	8.7
Spherical diam. –Å	38.3	33.4	27.6	21.4	22.5
Integrated intensity, $Q_0 \cdot 10^5$	21.3	16.7	9.54	5.73	2.32
Vol. fraction scattering, $(\Delta V/V) \cdot 10^3$	3.39	2.56	1.52	0.91	0.46
Fraction asphaltene sample scattering	0.42	0.32	0.19	0.11	0.06
Mol. wt. – vapor pressure osmometry	633.0	588.3	400.5	285.9	221.9
Mol. wt. – abs. X-ray intensity	1844.0	1175.8	528.3	274.3	159.1
Sample in solvent mixture*					
Size 1 particle diam. –Å	29.8	36.3	32.9	32.9	32.9
No. particles size 1/No. size 1	1.0	1.0	1.0	1.0	1.0
Size 2 particle diam. –Å	98.8	98.8	89.4	89.4	89.4
No. particles size 2/No. size 1	0.08	0.07	0.09	0.13	0.09
Integrated intensity, $Q_0 \cdot 10^5$	27.50	22.80	13.20	6.97	3.38
Vol. fraction scattering, $(\Delta V/V) \cdot 10^3$	3.66	3.04	1.76	0.93	0.45
Fraction of asphaltene sample scattering	0.46	0.38	0.22	0.12	0.06

*Solvent mixture is 90 wt.% tetralin, 2.5 wt.% *m*-cresol, 7.5 wt.% γ-picoline.

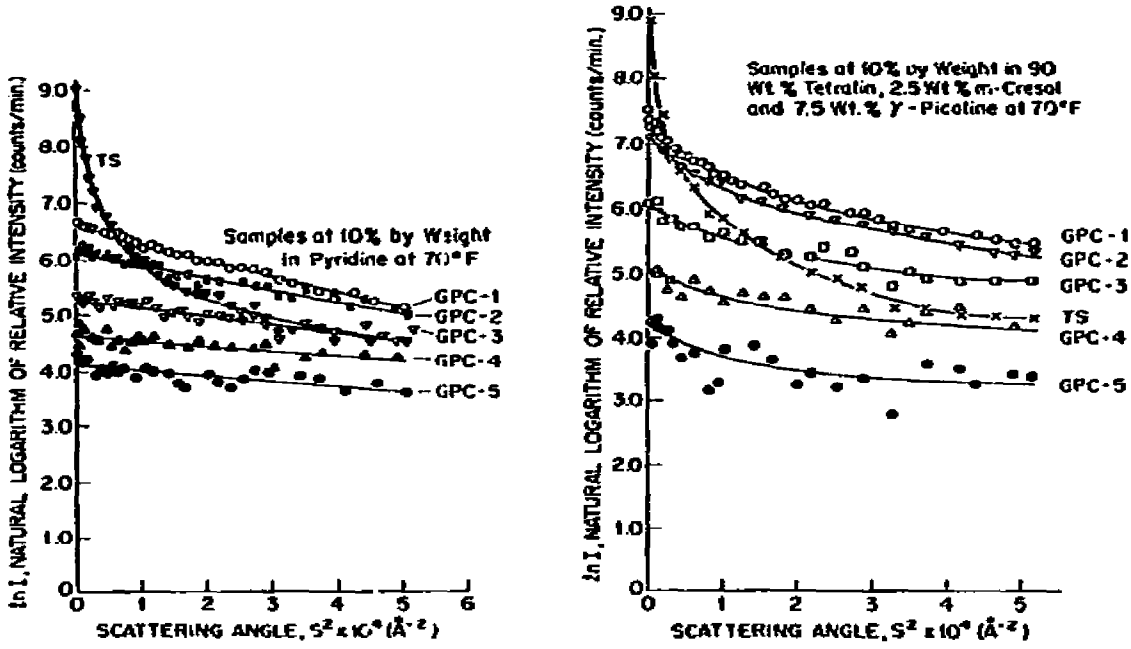

Fig. 7. Variation between the GPC fractions and the original sample when dispersed in pyridine at concentrations of 10 wt.% at 70°F.

Fig. 8. Variation between GPC fractions and the original sample when dispersed in a mixture of 90 wt.% tetralin, 2.5 wt.% *m*-cresol and 7.5 wt.% γ-picoline at concentrations of 10 wt.% at 70°F.

molecules, then an average of 5 GPC-1 molecules associate to form ~38 A particles and an average of 4 GPC-2 molecules associate to form ~33.4 A particles.

When dispersed in a mixture of 90 wt.% tetralin, 2.5 wt.% *m*-cresol and 7.5 wt.% γ-picoline, the GPC fractions form polydispersed systems. In each the particles were bimodally distributed with the preponderance of particles being the smaller of the two sizes. Tetralin is not as good a solvent as pyridine, *m*-cresol or γ-picoline and would be expected to permit the clustering of a few of the 30—36 A particles into 89—99 A particles. The Van der Waals attraction between the smaller particles would exceed the solvation repulsion of the solvent molecules. The fraction of the sample scattering X-rays is in each case higher in the solvent mixture than in pyridine.

GPC-4 fraction in pyridine at different concentrations

Scattering data are given in Fig. 9 for the GPC-4 fraction dispersed in pyridine at concentrations of 4, 10, 15 and 22 wt.%. Mie scattering is apparent in the 4 wt.% solution where the relative scattering intensity is

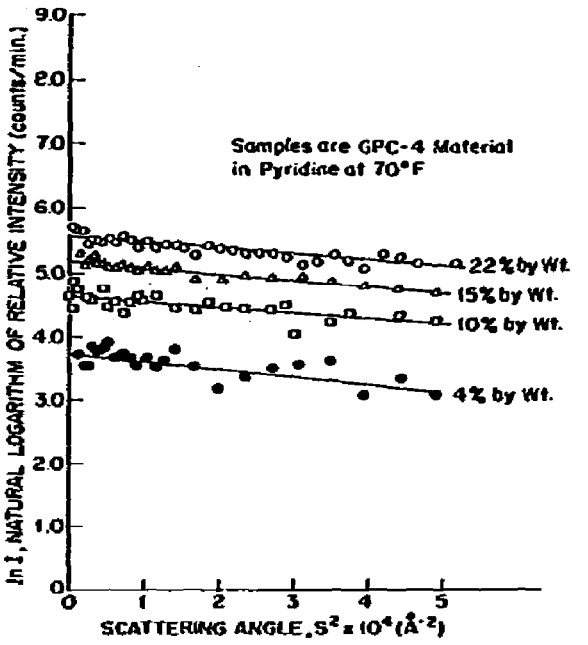

Fig. 9. Effect of the concentration of the GPC-4 fraction in pyridine at 70°F.

TABLE 4

Small angle X-ray scattering results for asphaltene fraction GPC-4 in pyridine at different concentrations at 70°F

Conc. wt.%	Conc. vol %	Solvent	Rad. gyration (Å)	$Q_e \cdot 10^4$	$(\Delta V/V) \cdot 10^4$	Fraction GPC-4 scattering
4	3.15	Pyridine	10.7	2.08	0.36	0.11
10	7.97	Pyridine	8.3	6.47	1.12	0.14
15	12.08	Pyridine	9.1	8.67	1.50	0.12
22	18.12	Pyridine	8.4	12.71	2.20	0.12
10	7.89	Mixture*	12.3	6.93	1.20	0.15
15	11.90	Mixture	10.2	10.11	1.75	0.15
22	17.72	Mixture	9.1	13.63	2.36	0.13

*Solvent mixture is 90 wt.% tetralin, 2.5 wt.% *m*-cresol, 7.5 wt.% γ-picoline.

relatively low. From the analyzed results in Table 4, it can be seen that the fraction of the sample scattering X-rays is nearly constant. One explanation is that only certain molecules are associating. When the concentration is doubled the number of particles double but the fraction scattering remains constant. The other explanation is that multiple scattering leads to an under-

estimate of the particle diameter and fraction scattering. The weight average molecular weight at the four concentrations was essentially constant, being 274±10. When the samples are dispersed in the mixture of solvents the particle diameters and fractions of the samples' scattering X-rays both increase.

GPC-4 fraction in different solvents

Scattering data are presented in Fig. 10 for the GPC-4 fraction dispersed in five solvent systems at a concentration of 10 wt.%. The relative scattering intensities are inversely proportional to the solvation repulsion of the solvent. The analyzed results are given in Table 5. With the exception of pyridine, the GPC-4 material formed polydispersed systems in the solvents. This can in part be attributed to the variety of compound classes in the sample. THF can solubilize hydrogen bonding molecules but has little influence on $\pi-\pi$ bonding molecules.

Effect of ultrasonic agitation

Runs were made with Tsf material at a concentration of 1 wt.% in pyridine to assess the effect of mechanical stress on the colloidal system. In one case the sample was allowed to remain at rest for at least 24 h and in the other the sample was ultrasonically agitated and immediately placed in the

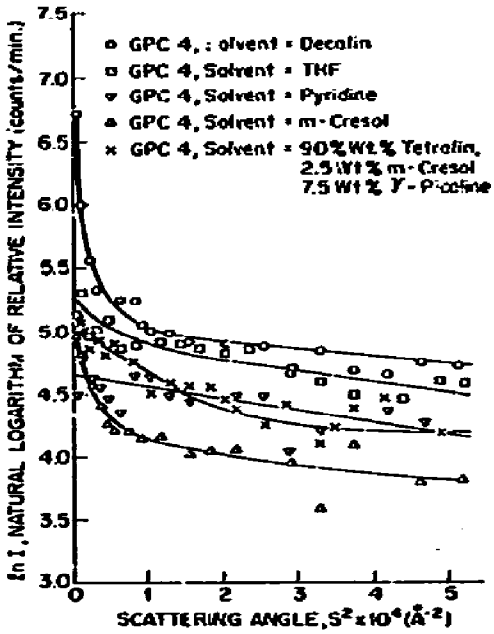

Fig. 10. Effect of solvent on GPC-4 fraction at 10 wt.% solutions, at 70°F.

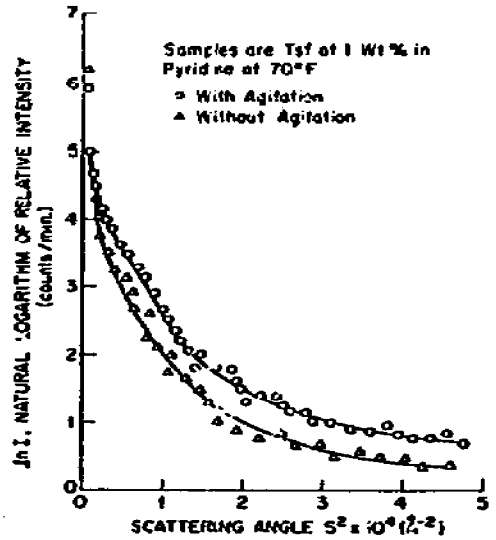

Fig. 11. Effect of agitation on the relative scattering intensity of Tsf in pyridine at a concentration of 1 wt.% at 70°F.

TABLE 5

Small angle X-ray scattering results for asphaltene fraction GPC-4 in various solvents at a concentration of 10 wt.% at 70°F

Solvent	Decalin	THF	Mixture*	Pyridine	*m*-Cresol
Size 1 particle diam., A	29.8	29.8	30.5	21.4	32.9
No. particles size 1/No. size 1	1.0	1.0	1.0	1.0	1.0
Size 2 particle diam., A	98.8	98.3	–	–	89.4
No. particles size 2/No. size 1	0.08	0.04			0.12
Size 3 particle diam., A	147.4	–	–	–	133.4
No. particles size 3/No. size 1	0.02				0.01
Integrated intensity, $Q_0 \cdot 10^5$	9.51	9.09	6.93	5.73	4.18
Vol. fraction scattering, $(\Delta V/V) \cdot 10^2$	1.57	1.37	1.20	0.90	0.61
Vol. % GPC-4 in sample	7.4	7.3	7.9	8.0	8.4
Fraction GPC-4 scattering	0.21	0.19	0.15	0.11	0.07

TABLE 6

Effect of agitation on small angle X-ray scattering by a high molecular weight asphaltene fraction at a concentration of 1 wt.% in Pyridine at 70°F

	With agitation	Without agitation
Size 1 particle diam., A	29.8	29.8
No. particle size 1/No. size 1	1.0	1.0
Size 2 particle diam., A	89.4	89.4
No. particles size 2/No. size 1	0.087	0.079
Size 3 particle diam., A	147.4	147.4
No. particles size 3/No. size 1	0.020	0.005
Integrated intensity, $Q_0 \cdot 10^5$	0.33	0.063
Vol. fraction scattering, $(\Delta V/V) \cdot 10^2$	0.0084	0.0016
Fraction asphaltene sample scattering	0.0105	0.0020

cell and the scattering curve obtained. The results shown in Fig. 11 indicate a higher relative intensity from the ultrasonically agitated sample. The particle size distribution and the volume fraction scattering results for the two systems are given in Table 6. Although the peaks in the particle size distributions are the same, approximately five times more of the Tsf material is scattering X-rays in the agitated sample. There is also more of the 147.4 A particles relative to the 29.8 A particles in the agitated sample. When the Tsf is allowed to rest, the larger colloidal particles apparently form a floc of the order of 1000 A or more. The floc will cause the Mie scattering that is observed and will reduce the number of particles scattering X-rays in the small angle range. When the agitated sample is allowed to rest for 24 h, the intensity of scattered X-rays drops again to the lower value.

CONCLUSIONS

The physical state of coal-derived liquid—solvent systems depends upon the balance of forces between molecules and associations of molecules at the temperature and shear state of the systems. At the molecular scale, the strongest forces of attraction are the $\pi-\pi$ bonding attractions between polyaromatic molecules. The force of attraction is usually greater when the polyaromatic molecules contain heteroatoms, such as phenolic oxygen and ring nitrogen atoms, which can hydrogen bond.

In all the systems studied, most of the colloidal particles were spherical with diameters in the range of 22—38 Å. These particles were formed by inter-molecular association of 3 to 5 polyaromatic molecules. The size of the particles formed by intermolecular association and the fraction of molecules associating into particles is closely related to the number average molecular weight of the unassociated molecules as shown in Fig. 12. Since the asphaltene and preasphaltene fractions are highly aromatic, the number of π-electrons in an individual molecule is also closely related to the molecular weight.

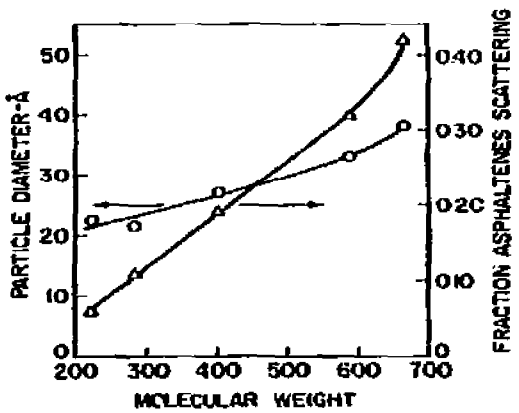

Fig. 12. Variation of the micelle diameter and fraction of the sample scattering X-rays with the number average molecular weight of the unassociated molecules in the 5 GPC fractions.

Once 3 to 5 molecules associate into a micelle, there appears to be little or no tendency for an isolated molecule to associate with the particle. The particle either has little or no residual capacity to $\pi-\pi$ or hydrogen bond with the molecule, or the molecule has considerably fewer than the average number of π-electrons and heteroatoms in the particular coal-derived liquid fraction. The solvent plays an important role through solvation repulsion. When dispersed in solvent molecules which are more easily "squeezed out", association of molecules with fewer π-electrons would be expected, Van der Waals attraction becomes important and polydispersed systems result.

The particle-size distribution data for the polydispersed systems indicate two or three separate peaks with a unique relationship between the sizes at which the peaks occur. Although the π—π bonding tendency between particles would be expected to drop off sharply, the London—Van der Waals attraction between particles would be expected to increase sharply as the size of the particles increases. The most stable orientation for particles held together by London—Van der Waals attractions would be as in a hexagonal close-packed arrangement as occurs when four 22—38 Å particles cluster as illustrated in Fig. 13 to form an 80—100 Å particle. The shape of the new particle is still approximately spherical. Depending upon the temperature, shear state and the properties of the "liquid" phase, further association could be expected to proceed in two ways. Four additional 22—38 Å particles could cluster with the 80—100 Å particle to form a nominally spherical particle of 130—160 Å or four 80—100 Å particles could agglomerate to form a super micelle or floc with a diameter in excess of 220 Å. Interestingly, the tendency to form spherical particles was observed by Ho [13] when asphaltenes were precipitated from an asphaltene—THF solution on the addition of decalin. Scanning electron micrographs as shown in Fig. 14 show the presence of spherical particles of 3000—4000 Å in diameter.

The limited data on the effect of concentration for the GPC-4 fraction shows that the fraction of the sample scattering X-rays is roughly independent of the concentration. Although this might appear to violate ther-

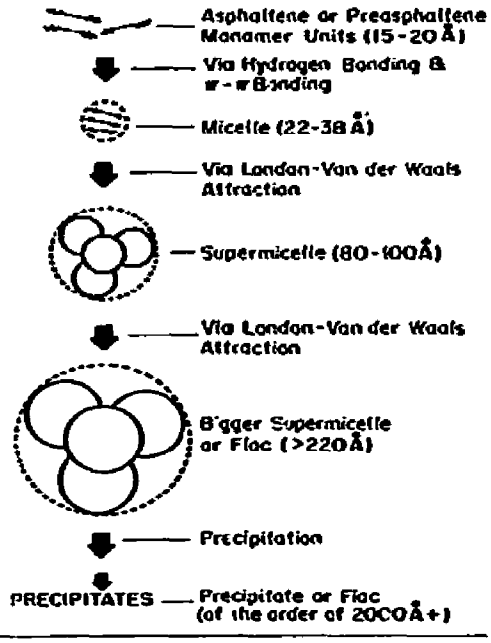

Fig. 13. Proposed association mechanism of asphaltenes and pre-asphaltenes in solution.

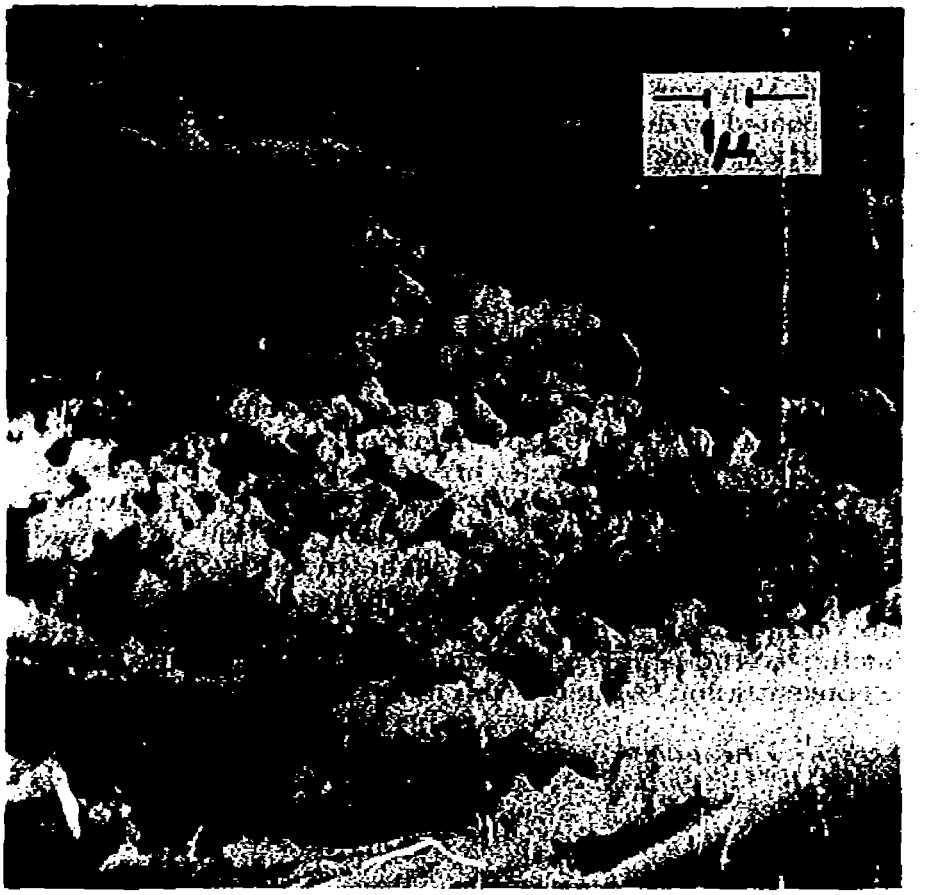

Fig. 14. Scanning electron micrograph at approximately 5000× of asphaltenes precipitated from an asphaltene-THF solution on the addition of decalin.

modynamic principles, this GPC fraction is a mixture of compounds with various tendencies to associate. The molecules which do have a strong tendency to associate, will, regardless of the concentration. When the concentration is increased, there is an increase in the solvation repulsion tendency through the presence of individual coal-derived liquid molecules in solution.

Floc structures with dimensions in excess of 1000 Å form when asphaltene-solvent systems are allowed to rest for extended periods. The existence of floc structures can be observed via Mie scattering and the structures are destroyed by mechanical shear as in ultrasonic agitation. Upon extended rest the floc structure returns.

ACKNOWLEDGEMENTS

The research reported here was sponsored under the U.S. Department of Energy Contact EX-76-5-01-2550.

REFERENCES

1 D.E. Briggs, D.V. Addington and J.A. McKeen, Coal IV, CEP Tech. Manual, 1978.
2 D.E. Briggs, Electrostatics in Non-Aqueous Liquid Particle Separations, (in press), Proceedings of Fine Particle Society Fall Meeting, 1980, Hemisphere Publ. Corp.
3 L.R. Snyder, J. Phys. Chem., 67 (1963) 2344.
4 B. S.-Y. Ho, Particle Size Configuration Determination of Coal-Derived Asphaltenes and Preasphaltenes in Solution by Small Angle X-ray Scattering, Ph.D. Diss., Univ. of Michigan (1930).
5 P.W. Schmidt and R.W. Hendricks, Acta Phys. Austraiaca, 26 (1967) 97.
6 P.W. Schmidt and R.W. Hendricks, Acta Phys. Austraiaca, 37 (1973) 20.
7 A. Guinier, G. Fournet, C.B. Walker and K.L. Yudowitch, Small Angle Scattering of X-rays, Wiley, New York, 1955.
8 W.W. Beeman, P. Kaesberg, Anderegg and Webb, Handbuch der Physik, 32, Springer-Verlag, Berlin, 1957.
9 M.H. Jellinch, E. Solomon, and I. Fankucken, Ind. Eng. Chem. Anal. Ed., 18 (1966) 172.
10 G.G. Vonk, J. Appl. Crystallogr., 9 (1976) 433.
11 O. Kratky in: T.A.V. Butles, H.E. Huxley and R.E. Zirkle (Eds.), Progress in Biophysics and Molecular Biology, 13, Pergamon Press, New York, NY, 1963.
12 O. Kratky, "Application of the Lupolen Platelet Designated with 16/12 as a Calibration Sample for the Determination of the Absolute Intensity and of the Primary Energy in the Case of Slit-Collimation," unpublished paper, (1977).
13 D.E. Briggs, B. Ho, P.A.S. Smith, et al., "Physical and Chemical Behavior of Liquefied Coal in Solids Separation," U.S. DOE Report FE-2550-8, Aug., 1979.